Physical chemistry in foam drainage and coarsening

Arnaud Saint-Jalmes†

Received 15th May 2006, Accepted 19th July 2006
First published as an Advance Article on the web 8th August 2006
DOI: 10.1039/b606780h

This review covers recent advances in the study of foam drainage and coarsening, focusing especially on the effective role of the foam chemical components on those aging processes. The determination of the relevant parameters controlling foam drainage and coarsening today remains a major issue: are the physical parameters (like bubble size and liquid fraction) sufficient to define a foam and to predict its evolution, or do the chemical components also matter? And if these foam components are important, one has to determine by which mechanisms, and which microscopic parameters involved in these mechanisms are eventually crucial. I report here recent experimental results, shedding light on these issues. It allows us to summarize how the surfactant, the liquid bulk properties, and the gas modify or not the drainage and coarsening features. The coupling between drainage and coarsening is also discussed, as well as the role of the experimental conditions (sample height, shape or foam uniformity).

1 Introduction

When dispersing a gas into a liquid, one can eventually create a foam.[1–3] But such a foam will be highly unstable, and will probably survive for only a few seconds. Another ingredient—usually some soap, or surfactant, dissolved into the aqueous phase—is required to produce a stable foam, which can stand for hours. The presence of these molecules adsorbed at the gas–liquid interfaces provides the foam stability, both by reducing the gas–liquid surface tension γ, by modifying the viscoelasticity of these interfaces, and by inducing repulsive forces between bubbles.[4–6]

A foam consists of bubbles compressed on each other (Fig. 1): the degree of packing can be characterized by the liquid volume fraction, $\varepsilon = V_{liq}/V_{foam}$ (with V_{liq} the volume of liquid dispersed into a foam volume V_{foam}). For low liquid fraction ($\varepsilon \leqslant 0.05$), the bubbles are polyhedral, with slightly curved faces, and well defined edges (see the top part of the foam in Fig. 1). Increasing the amount of liquid in a foam decreases the amount of packing, and at $\varepsilon_c = 0.36$ (random close packing of solid spheres) bubbles are no longer deformed. With the liquid fraction, the bubble size is a second crucial parameter to define a foam. It can be defined by its sphere-equivalent radius R, diameter D or by the bubble edge length L (easier to determine for dry foams). Relations can be found between L and D, depending on the bubble shape and number of faces: for instance, a simple bubble geometry, known as the Kelvin geometry, is often used to model bubbles, and for which one gets $D = 2.7L$ (Fig. 2). In case of a

Laboratoire de Physique des Solides, Université Paris-Sud, Orsay, France. E-mail: saint-jalmes@lps.u-psud.fr
† *Present address*: Groupe Matière Condensée et Materiaux, Université Rennes 1, Rennes, France.

Arnaud Saint-Jalmes

Arnaud Saint-Jalmes got his PhD in 1997 on the subject of Langmuir monolayers at the ''Laboratoire de Physique Statistique'' of the Ecole Normale Supérieure in Paris. He then spent two years with D. Durian at UCLA (Los Angeles), where he began to get interested in aqueous foams. Back in France, he obtained a staff position (CNRS) at the ''Laboratoire de Physique des Solides'', in Orsay, near Paris, continuing his studies on foams and liquid surfaces. In early summer 2006, he moved to the ''Groupe Matière Condensée et Matériaux'' at the University of Rennes (France).

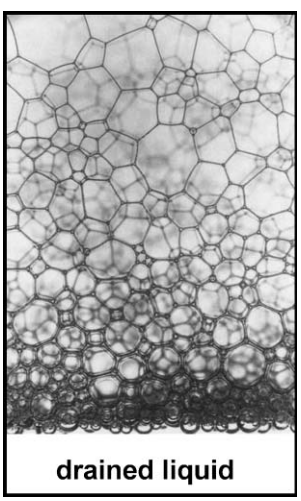

Fig. 1 A foam after drainage, at equilibrium. The network of Plateau borders and nodes is clearly seen, as well as the wet foam layer due to capillarity in contact with the drained liquid. At the top, the foam is very dry ($\varepsilon < 0.01$), and the bubble are polyhedral, while the bubbles of the first layer of the foam–liquid interface are spherical, and locally $\varepsilon = 0.36$.

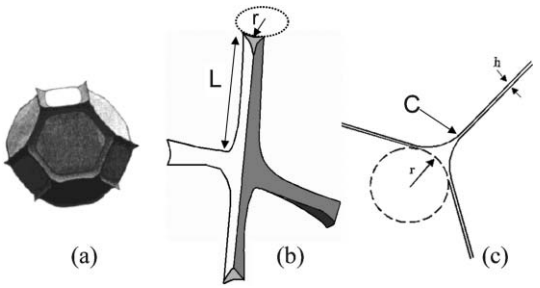

Fig. 2 (a) The shape of the Kelvin bubble (adapted from ref. 8), (b) drawing of four Plateau borders (PBs) attached by a node, and definition of the PB length L, and PB radius r, (c) cross section of a Plateau border, with the three films attached to it at points C.

polydisperse foam (with bubbles having many different diameters), which is the case in most of the experiments and applications, mean values are used, or even higher order of the bubble radius distribution, like the Sauter radius, $R_{32} = \langle R^3\rangle/\langle R^2\rangle$. Besides these physical parameters (bubble diameter and liquid fraction), one can completely describe a foam if one knows which surfactants adsorbed at the gas–liquid interfaces are used, how they modify the interfacial properties, and what are the bulk properties of the surfactant solution and of the gas used. A main question is then: does one need to know all this information to explain the foam behavior? In other words, what are the relevant parameters to define a foam? For simplicity, in the following, we always call 'surfactants' the molecules adsorbed at the interfaces, though foams can be made not only with low molecular weight surfactants (like the very common sodium dodecyl sulfate, SDS); more complex molecules, like polyelectrolytes or proteins, can also be used to produce stable foams.

Considering only the fact that a foam is basically a large volume of a gas, mixed with a much smaller amount of a fluid, the properties of the resulting material thus appear quite curious, either on the optical, electrical, thermal or mechanical point of view.[1–3] Moreover, these properties can be easily tuned, and even inverted, by modifying the foam physical or chemical parameters: a foam can be opaque or transparent, fluid-like or solid-like, conducting or insulant. Such a wide range of possible different behaviors is at the origin of the use of foams in many industrial applications,[1–3] and also why scientists are still excited by these materials, and keep struggling with them on many fundamental issues.

A crucial feature of aqueous foams is that they irreversibly evolve in time: foams ''drain'', ''coarsen'', and finally completely collapse as the films between bubbles rupture.[1–3] Due to gravity, the liquid and gas in the foam tend to separate: with time, the liquid leaks out of the foam, and the foam becomes dryer. This effect, known as drainage, is the subject of Section 2. Also, with time, the mean bubble diameter increases due to gas diffusion between bubbles; results on this foam coarsening are reported in Section 3. Both effects can occur on the same timescale and can thus be coupled (Section 4).

The main objective of this article is to review recent experimental and theoretical results showing if and how drainage and coarsening depend on the foam components. If so, the problem is then to identify by which mechanism, and which parameters, modified by the components, are involved. In that spirit, it then becomes possible to compare the importance of these changes to those induced by the physical parameters (bubble diameter D, liquid fraction ε), or to those due to the experimental conditions. In order to present these results, only the basic physical concepts needed are recalled, as the goal here is not to give a detailed presentation of the theories of drainage and coarsening. Also, the problems of determining why a solution foams or not (foamability or foaminess) are not discussed here. Only solutions which are already foaming well, and which contain enough foaming agents are considered: we focus here on the time evolution of such foams. This also means that thin films between bubbles are always rather stable, so that spontaneous thin film ruptures do not occur during the foam aging, and that they finally break on a much longer timescale than those of drainage and coarsening. Lastly, the images and graphs shown here are selected to illustrate as best as possible known results found in the literature.

I will show here that there is not a simple and unique answer to these issues on the effective contributions of the chemical components: the components are sometimes found to be really important, while almost irrelevant for other properties. The point is that we are starting to understand better how and why, and a clearer picture of the balance between physics and chemistry in foams is emerging, though one must also admit that many questions remain unsolved.

2 Drainage

2.1 General concepts

Expressed in a simple manner, the main objective of drainage studies is to find out how long it takes for a foam sample to drain. To determine at which velocity the fluid is draining in the foam, and a typical drainage time, the first step is to describe the fluid distribution within the foam. The liquid is confined into a network of channels (named Plateau borders, PBs), which are connected at nodes in fours (Fig. 2); also, some liquid is trapped in the thin and flat films formed between two bubble faces. The PBs, which decorate the bubbles on their edges, as seen in Fig. 1 and 2, have a specific triangular-like section A; in the following, we call L their typical length, r their radius of curvature, and $A = cr^2$ (with $c \approx 0.161$).[2,7,8] After comparison of the amount of liquid in PBs, nodes and films, a simplification is usually made: the volume of liquid contained within the PBs is always considered much bigger than the that in the nodes and in the films. In that respect, the liquid fraction is the volume of liquid inside the PBs decorating a bubble divided by the bubble volume; taking into account the details of the bubble geometry, one finds $\varepsilon = \delta(r/L)^2$, with $\delta = 0.17$.[2,8] This assumption is quite helpful to analytically derive drainage models, but is expected to be valid only for dry foams, up to $\varepsilon \approx 0.05$. With this assumption, the PB section A is simply proportional to ε: as a foam drains, the PBs shrink and their sections decrease.

In this network of PBs, gravity makes the fluid flow downward. The liquid also flows because of capillary effects, which are related to liquid fraction gradients. Such gradients of ε imply pressure gradients in the liquid.[2,7,8] In a wet part of

the foam, the PB radius is bigger than in a dryer part: due to the Laplace–Young law, the capillary pressure in the liquid in the wet part must be higher than in the dry part.[2,7,8] Thus a capillary flow is induced, bringing liquid from high ε regions to regions with low ε. In that sense, one can see that capillary effects tend to smooth out liquid fraction gradients. The resulting steady state flow in a foam is obtained by balancing these gravity and capillary effects with some viscous dissipation occurring within the fluid network.

Finally, it is important to introduce another basic point here. Drainage does not make all the liquid leak out of a foam: an equilibrium state is previously obtained, implying that some liquid is kept inside the foam. For a foam sitting on its drained liquid (as in Fig. 1), an equilibrium is found between capillary effects, which tends to suck liquid from the underneath pool, and gravity. Right at the interface, the bubbles are spherical (Fig. 1) and the liquid fraction is $\varepsilon_c = 0.36$ (random close packing of non deformed spheres). There is thus always an equilibrium capillary liquid holdup in a foam: it implies the existence of a very wet foam layer at the foam bottom. Its typical length is $\xi = \gamma/\rho g D$, and it is the length over which the liquid fraction varies from 0.36 to 0.18 (ρ is the surfactant solution density, and γ is the surface tension). In Fig. 1, with bubble diameters of approximately 1 mm, this length is about 2–3 bubbles high.

2.2 Theoretical background

Drainage models are based on the formalism developed for porous media. These models use Darcy's law, which relates the liquid velocity to the driving pressure gradient $\boldsymbol{G}$ (including both gravitational forces ρg, and capillary pressure gradients) *via* the permeability k and the fluid viscosity μ: $\boldsymbol{G} = \mu v/k$. In this approach, the foam is considered as an effective medium. However, as discussed below, to determine the form of k, one has to elucidate the details of the flow on the scale of a single PB and node. A major difference with solid porous media is that the pore size (the PB section, A) is dynamically coupled to the liquid fraction (as noted before, $A \sim \varepsilon$): Thus, the permeability k is a function of liquid content, $k(\varepsilon)$. Note that the inverse of the permeability can be seen as a hydrodynamic resistance R. The foam drainage equation is then derived by injecting the velocity obtained from the Darcy's law into a continuity equation, $\frac{\partial \varepsilon}{\partial t} + \nabla\cdot(\varepsilon v) = 0$. One then gets the following equation, describing the time and space variation of $\varepsilon(\boldsymbol{r},t)$, discussed in such general form in ref. 7–10 (with operators acting on the spatial coordinates):

$$\frac{\partial \varepsilon}{\partial t} + \nabla\cdot\left(\frac{\rho g}{\mu}\varepsilon k(\varepsilon)\right) - \nabla\cdot\left(\frac{\gamma\sqrt{\delta}}{2\mu L}\frac{k(\varepsilon)}{\sqrt{\varepsilon}}\nabla\varepsilon\right) = 0 \qquad (1)$$

The next step is then to determine the form of $k(\varepsilon)$. Assuming immobile PB surfaces, a Poiseuille flow is obtained inside these solid tubes, and this means strong viscous dissipation (or high hydrodynamic resistances). In this case, $k(\varepsilon) = K_c \varepsilon L^2$. Many pioneering works dealt with this case.[7,11–15] Here K_c is a dimensionless number, describing the PB permeability; also, one can define a PB hydrodynamic resistance $R_c \approx 2/K_c$.[8] For the drainage velocity, it is worth noting that in a steady-state—constant liquid fraction and no capillary effects—one gets a simple relation between v and k:

$$v = K_c \rho g L^2 \varepsilon/\mu \qquad (2)$$

From this equation, one can already note the important role of the bubble diameter and of the bulk viscosity, which sets a velocity scale $v_0 = \rho g L^2/\mu$. In a foam, this typical velocity is finally weighted by the permeability constant and the liquid fraction to get the actual fluid velocity. Quantitatively, for immobile PB walls, the value of K_c depends only on the PB geometry, and numerical simulations give $K_c = 1/150 \approx 0.0067$. This drainage regime is called the "channel-dominated" regime.

Regarding the localization of the dissipation, another case is possible. If the viscous dissipation in the PBs turns out to be less than that inside the nodes, another form for $k(\varepsilon)$ is expected: $k(\varepsilon) = K_n\sqrt{\varepsilon}L^2$. In that case, in steady-state (ε = constant):

$$v = K_n \rho g L^2 \sqrt{\varepsilon}/\mu \qquad (3)$$

This regime, known as the "node-dominated" regime, was first introduced and studied in detail in ref. 8,16. Again, K_n is a dimensionless number, describing the node permeability, with an associated node resistance $R_n \approx 1/K_n$.[8] Even though most of the liquid is still within the PBs, the viscous dissipation can be bigger in the nodes if the flow in the PBs is more plug-like than Poiseuille-like (as proposed in ref. 8,16); in that case the PB surfaces are flowing with the bulk liquid, producing much less hydrodynamic resistance in these PBs. The value of K_n is expected to be of the same order of magnitude as K_c.[8,17]

In a foam, viscous dissipation occurs both in the PBs and in the nodes, and to determine the drainage regime and the foam permeability k, the balance between dissipation in PBs and nodes must be considered. It has been proposed to treat the PBs and nodes as resistances mounted in series, implying that:[10]

$$L^2/k(\varepsilon) = 1/\varepsilon K_c + 1\sqrt{\varepsilon}K_n \qquad (4)$$

Quantitatively, the foam permeability k first depends on the shape of the PBs and nodes, *via* the values of K_c and K_n. But, as pointed out previously, the balance between dissipation in PBs and in nodes has to depend also on the type of flow through these structures, and consequently on the velocity at their walls. There is indeed some possible coupling between bulk and surface flows inside the PBs and nodes: their walls are simply the gas–liquid bubble interfaces, having their own complex rheological properties. A first possible coupling is based on the fact that the PB walls can be sheared by the bulk flow. This shear results from non constant velocity along the perimeter of a PB section: one considers here that the velocity in the 3 corners where the PB is connected to thin films (point C in Fig. 2c) is zero, whereas it is dependent on the bulk flow along the free surfaces, in between the PB corners. This coupling is characterized by a dimensionless number M: $M = \mu r/\mu_s$ (with μ_s, the surface shear viscosity). This parameter M defines the interfacial "mobility", and was initially introduced by Leonard and Lemlich.[18] Using the Kelvin

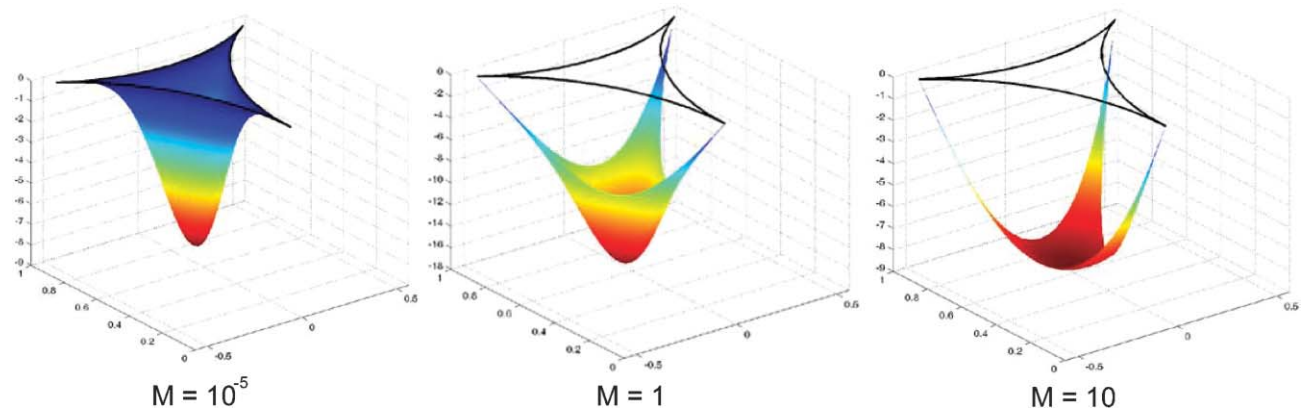

Fig. 3 Simulations illustrating the surface–bulk flow coupling in a PB: fluid velocity profiles in a cross section of a PB, for 3 values of the mobility parameter M. On the left, the surfaces are immobile and do not flow with the bulk liquid, while it is the opposite for $M = 10$, where the surfaces are highly strained and sheared by the flow.

bubble geometry and the previous assumption of a low liquid fraction, it can also be written with the bubble diameter and the liquid fraction: $M \approx 0.9\mu\sqrt{\varepsilon}/\mu_s$. Taking this coupling into account modifies the PB permeability K_c, which becomes an increasing function of M (or inversely, the PB resistance R_c decreases with M). The exact form of $K_c(M)$ was first numerically calculated,[18–20] and more recently analytically derived by Koehler *et al.*,[21] who studied in detail the different possible flow cases in PBs, and in films. In agreement with this work, in Fig. 3 we show simulations of the flow pattern inside a vertical PB at 3 values of M. For $M = 10^{-5}$, meaning for instance a very high surface shear viscosity, the surfaces are immobile and strong velocity gradients are found within the velocity profile; this corresponds to the maximum value of hydrodynamic resistance in the PB. As M increases, one can see that the surfaces start to flow with the bulk liquid, and that there are fewer and fewer velocity gradients. For $M = 10$, the velocity is almost the same in the PB center and at its surfaces (except in the corner points C), and the PB offers practically no more resistance to the flow. Here the velocity is kept to zero in the connected thin films, which sustain the foam structure and the weight of the flowing liquid. A dependence of the node permeability K_n with M is also expected. However, due to the node complex geometry, this is less well understood, and simulations are in progress to elucidate the detailed form of $K_n(M)$. In ref. 17, it is shown that for low M, the nodes can be considered as tiny corrections of the PB length (their contribution to dissipation is thus low and on the order of r/L when compared to that of the PBs); however, for high M, a node resistance value is found of the same order of magnitude as the PB resistances. Thus one can deduce that the node resistance R_n must increase with M. In fact, one way to understand this result is to see the nodes as bigger and bigger obstacles to the flow as M increases. Since this coupling described by M implies that R_c decreases with M, and that R_n increases with M, one can predict a crossover from the channel-dominated regime to the node-dominated regime as M increases, and with M as the relevant control parameter.

Another surface–bulk coupling is possible in the fluid network, and is related to the creation by the bulk flow of interfacial surface tension gradients.[22] The balance between bulk and surface effects is then described by $N = (\mu D_{ef})/(Er)$, where D_{ef} is a diffusion coefficient containing both surface and bulk diffusion coefficients of the surfactant, and E is the Gibbs elasticity of the interface.[22] Considering this coupling, and dealing only with a simplified PB cylindrical shape, it has been showed that a drainage transition can occur as N is varied: at low N, $k(\varepsilon) \sim \varepsilon$, as for immobile surfaces; while at high N, $k(\varepsilon) \sim \varepsilon^{1/2}$. Thus, for high N, and without requiring the presence of nodes, a similar form to the one predicted for high dissipation in nodes is found. Obviously, this coupling can also occur in the nodes, and the node permeability might also change with N. Note that this coupling was also discussed regarding the drainage of single thin films.[23,24] Lastly, other interfacial parameters, like the dilational viscosity might also matter, though they do not appear explicitly in M or N.

In these last years, a theoretical framework has been developed: it can be summarized by eqn (1) and (4), together with the fact that K_c and K_n are functions of M and N. These models show both that the drainage velocity depends on the physical parameters like the bubble size and liquid fraction, but also that bulk viscosity and the surfactants (*via* the shear viscosity, or *via* surface elasticity) should play a role. The question is now to check which of these ideas are consistent with experiments, and if the assumptions made in the models are verified.

2.3 Experimental approaches

2.3.1 Concepts and procedures. With 3D macroscopic foams, different types of experiments can be done to study drainage. Obviously, the observation of the drainage of a standing foam (free-drainage) is conceptually the most simple case. In this procedure, one can measure the volume (or height) of liquid drained with time $V(t)$, or the decrease of the local liquid fraction at a given position (see below for methods of liquid fraction measurements). However, the free-drainage case is not as simple as it might look. For direct comparisons to models, it first requires a controlled and reproducible initial state at time t_0. This means that the foam must be uniform and with a constant liquid fraction all along its height; this is indeed not easy to produce, especially for high liquid fractions. Moreover, free drainage also often requires long experimental times, to follow the dynamics up to the final equilibrium state,

and on such long timescales coarsening might interfere with drainage, as discussed in Section 4. Finally, the presence of the capillary liquid holdup at the foam-liquid interface add some non trivial boundary conditions.

Forcing the surfactant solution at a controlled flowrate Q into a initially drained and dried foam (''forced-drainage'') turned out to be a simple and useful technique to study liquid transport in foams.[25] The result of gravity and capillarity effects, acting there in the same downward direction, is the existence of a well defined front, moving downward at a constant speed v. Mass conservation implies that $\varepsilon v = Q/S$ (where S is the section of the container) and ε is the liquid fraction above the front. Knowing Q, and measuring v, one can then obtain relations between v, ε and Q (without dealing with boundary conditions at the bottom or top container, and on short experimental timescales). A variant of the forced-drainage procedure is the pulsed-drainage one, where only a given volume of liquid is injected. However, there is an important limit with forcing liquid into a foam: as Q is increased to attain wetter foams, a bubble position instability occurs, which limits the possible range of the liquid fraction. Above a critical liquid fraction ε_{crit}, the PB skeleton can no longer sustain the flowrate, and some bubbles start to flow downward with the liquid, whereas others consequently rise upward. Different types of convective bubble motions have been observed,[26,27] even associated with size segregation, and depending on the shape of the foam container. Results show that the critical liquid fraction decreases with increasing the bubble diameter.[26] These instabilities are striking for many reasons: first, the value of ε_{crit} is low ($\varepsilon_{crit} = 0.1$ for 1 mm bubble diameter, for instance) and this value is difficult to explain (it is always well below $\varepsilon_c = 0.36$, where the bubbles are no longer packed, and become free to move). Also, within a convective roll, foams at different liquid fractions are flowing side by side: at a given horizontal section, such gradients should not be stable because of capillarity. It has been recently proposed that dilatancy could be an important ingredient in this problem explaining how foam at different liquid fractions can coexist.[28,29]

Experiments can also be done at the scale of a single PB, rather than in macroscopic foams where one measures average values. In ref. 30,31, Koehler *et al.* add tracers to the fluid, and use confocal microscopy to measure the velocity profile inside a PB embedded into a foam. One can also create a single PB, held on a solid frame and study its shape and section variation with flowrate, as well as the pressure drop associated.[32,33] Lastly, another simple geometry can be used: by injecting some surfactant solutions at a controlled flowrate Q between two glass plates, one can create two ''pseudo-PBs'' or ''surface PBs'' (with one of their three sides on the glass plate) connected by a single film.[34] Here also, it is possible to optically measure the section as a function of the flowrate Q.

2.3.2 Methods of liquid fraction measurements. The foam optical properties strongly depend on the liquid fraction. As soon as a foam has many bubbles in thickness, it usually appears as a white material, like milk, because the light entering the foam is multiply scattered. In that limit of multiple scattering, the light propagation is diffusive, and is characterized by a light mean free path, l^*. The transmitted light I_T is then proportional to l^*/T, where T is the sample thickness.[35] The light mean free path l^* decreases with ε: this means that the wetter the foam, the darker it looks in transmission. In Fig. 4, we show different examples in free and forced drainage based on the measurements of the transmitted light. As seen in this figure, it allows to qualitatively evidence gradients of ε, and to measure their evolution with time. In free-drainage (Fig. 4a), one can see that the foam gets dry from the top down, with a ''dry front'' moving downward. In this situation, gravity and capillarity act in opposite directions, which make the liquid fraction gradient more and more spread with time. In forced-drainage (Fig. 4b), a sharp front is observed: it keeps a constant shape, which mathematical form is discussed in ref. 7,8. Thus, this light transmission technique is accurate to determine liquid fraction gradients, front position and speed, but it remains difficult to use it regarding the quantitative estimation of ε, as the details of light transport in foams (concerning for instance the dependence of l^* with ε) are not yet well understood (complex effects like photon channeling within PBs[36] occur and need to be taken into account). When the conditions for multiple light scattering are not obtained, the front speed can still be measured optically by adding some fluorescent probes in the injected fluid, but this requires only a few bubbles in the thickness sample.[8,16]

The foam electrical properties are also used to measure the liquid fraction. A foam can be modeled as a R–C circuit in parallel, with the foam conductivity being proportional to the liquid fraction. Initial studies showed that this proportionality can be used to follow forced-drainage fronts, and some models

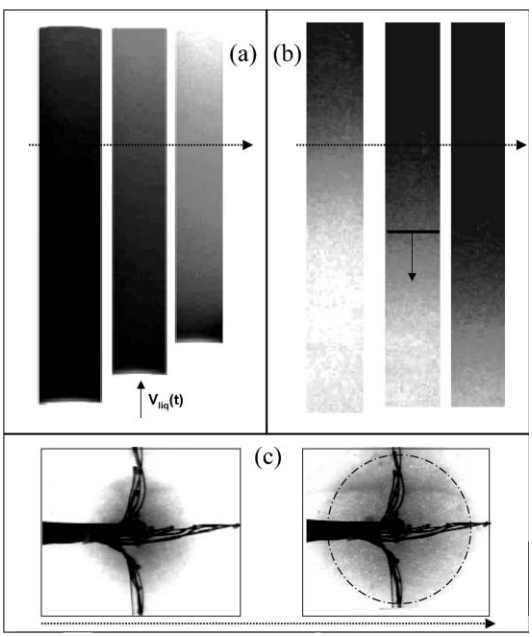

Fig. 4 Transmission pictures of foam during drainage. The dashed arrows indicate the time increase: (a) free-drainage at three different times, (b) forced-drainage at three different times, and (c) forced-drainage in microgravity conditions. In (c), the liquid is injected inside a dry foam, at a single point, at the cell center; electrodes and their wires for conductivity measurements are also seen, placed on a cross centered on the injection point.

were proposed for the relation between ε and the conductivity of the foam.[37,38] Note that front detection based on capacitance measurements was also performed.[39] Recently, with new measurements on foams at high liquid fractions, and gathering results obtained from different dispersed systems, a calibration curve has been proposed which gives the relation between the liquid fraction ε and the relative conductivity of the foam $\sigma = \sigma_{foam}/\sigma_{solution}$:[40]

$$\varepsilon = 3\sigma(1 + 11\sigma)/(1 + 25\sigma + 10\sigma^2) \quad (5)$$

This equation is valid over the whole range of ε and σ, both ranging from 0 to 1. Electrical conductivity measurements turn out to be very useful to quantitative local measurements, in free or forced-drainage. Lastly, it has to be noted that the use of techniques like NMR or electron spin resonance (ESR) for foam drainage studies has been tested.[41]

2.4 Recent results on the role of components

In this section, we consider that the bubble size is constant with time, and that no coarsening (nor spontaneous film rupture) occurs during drainage. The case of simultaneous drainage and coarsening is treated in Section 4.

2.4.1 Effect of the surfactants. Using the forced-drainage method, results showing the existence of different drainage regimes have been obtained by varying either the bubble size or the surfactants.[8,16,25,42–45] In Fig. 5, we show typical data illustrating a major result of these forced-drainage studies: the graph reports the liquid velocity as a function of the liquid fraction for a fixed bubble size (D = 2 mm), fixed bulk viscosity, and for foams made either of a solution containing sodium dodecyl sulfate (SDS) or made of a solution containing a milk protein (casein). Some protein solutions can foam, and interfaces covered by proteins usually have much higher interfacial elasticities and viscosities than surfactant layers.[46] For a small surfactant, v is proportional to $\sqrt{\varepsilon}$ (consistent with the node-dominated regime, eqn (3)), while $v \sim \varepsilon$ for the protein foam (as predicted for the channel-dominated regime, eqn (2)). In these last years, experimental results have clearly shown that drainage rates and regimes depend on the surfactant, and thus on the interfacial properties.

In ref. 45, forced-drainage experiments over a wide range of bubble diameters and for various surfactants are reported: permeabilities K_c and K_n, and resistances R_c and R_n, are extracted from the data, using the model of PBs and nodes in series (eqn (4)). It appears that these values are not constant and depend on the system and bubble size. Comparisons of these data to the model predicting the evolution of K_c (or R_c) with M are done by considering the surface shear viscosity μ_s of the different solutions as the only adjustable parameter. It turned out that a good agreement can be found between the data and this model, and that the deduced surface shear viscosities are quite correct. In Fig. 6, the measured R_c and R_n are presented: once plotted *vs.* M, a simple picture emerges, with two well defined extreme regimes. At low M, a channel-dominated regime is found, and at high M, a node-dominated regime occurs. In the intermediate range $0.8 < M < 3$, precisely when the drainage curve exponent α ($v \sim \varepsilon^{\alpha}$) is neither 1 nor 1/2 and that a couple (R_c, R_n) are deduced from the data, these values of R_c and R_n turn out to be almost equal; in fact, one finds R_n slightly above R_c, consistent with making the PB and node contributions equal in eqn (4). Clearly, R_n is found to increase with M and to depend on the conditions (considering it as a constant does not permit quantitative interpretation of correct data[47]). The results shown in Fig. 6 are also confirmed by those of ref. 43 corresponding to $M \approx 1$, and for which the node and PB resistances are also found quite similar. Also, experiments on single PBs confirm the relevant role of the coupling described by M. Surface shear viscosities

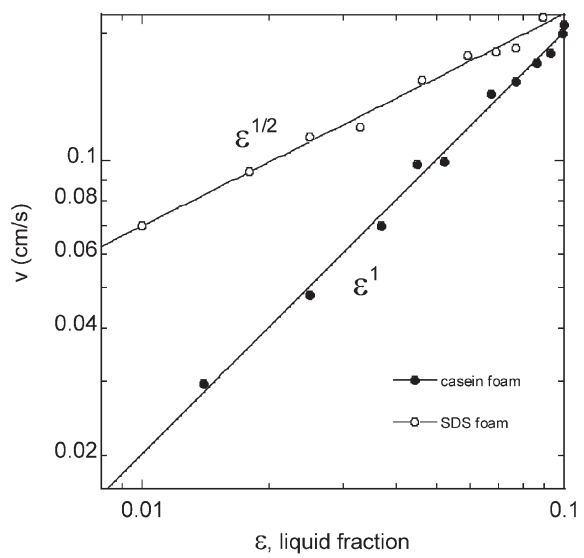

Fig. 5 Typical forced-drainage curves, illustrating recent results described in the text. Here, the bubble size and bulk viscosity are constant, and only the interfacial properties are different (foams are made from a SDS solution, and from a casein solution).

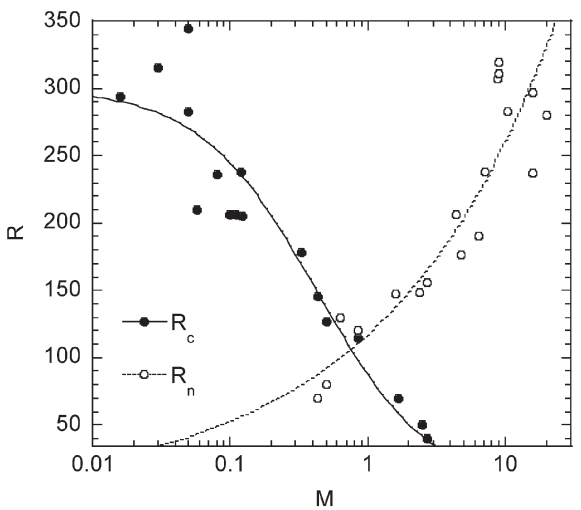

Fig. 6 PB and node resistances as a function of the mobility parameter M: a crossover is observed in the range $0.8 < M < 3$. At low M, one finds the "channel-dominated" drainage regime, and at high M, the "node-dominated" regime. The solid line through the PB resistance R_c is the model described in ref. 21, while the dashed line through R_n is just a guide for the eyes.

μ_s are also deduced from the measurements of the flow profile inside a PB,[31] or from the PB section and pressure drop.[32] All these methods give values in fair agreement, and also within the range found in the literature (measured by other methods).[48–53] For high values of surface viscosity $\mu_s \approx 10^{-2}$ *g/s* obtained typically for protein layers, all the measurements agree quite well, whereas for interfaces covered by a low molecular weight surfactant, like SDS, the dispersion of the measured values is still large, probably because the μ_s values are quite low ($\sim 10^{-5}$ *g/s*), close to the accuracy of the methods and because decoupling bulk and surface flow is complex in that case. In that spirit, the measurements based on foam drainage might be more accurate since they are directly based on this coupling, and deduced from it. Note also that for the case of SDS solutions, uncontrolled traces of dodecanol or of other impurities can also be responsible of the observed discrepancies.

From all these measurements, it seems that the mechanism linked to M, at least when M is varied by D and the surfactants, is relevant in foams. The quantitative agreement, *via* the correct values of μ_s, validates the assumptions made in the models, especially some geometrical constants describing the shape of PBs and nodes. In that sense, studying foam drainage appears to be a way to scan the geometrical structure of a foam. One can then also wonder if all the other assumptions of the model can be verified. As stated previously, drainage models are supposed to be valid only for low liquid fractions: by forced-drainage experiments, due to the convective instabilities, ε only goes up to around 0.15, and at these values it seems that the models are still correctly describing the data (a way to reach higher values of ε is discussed in Section 2.5). It is also assumed in the mechanism linked to M that the thin films are neglected, and that consequently the velocity is zero at the film–PB junctions (point C, Fig. 2c). In fact, experimentally, different situations can be found depending on the bubble diameter D: for a fixed ε, D sets the PB radius r, and thus the range of capillary pressure $P_c \sim \gamma/r$ at which the PBs suck the liquid from the films.[4,5] The PB radius also sets the maximum fluid velocity v, and the capillary number $Ca = \mu v/\gamma$ describing the balance between inertial and capillary effects. For D typically below 1 mm and for ε of ~ 0.01, the capillary suction from the PBs is high ($P_c >$ 100 Pa): under such a pressure drop, usually surfactant films thin down rapidly to a thickness of a few tens of nm. Secondly, the capillary number is small ($\sim 10^{-6}$), showing that the dynamic effects due to the liquid flow are low (quasistatic limit). Both of these facts imply and confirm that, for these conditions of small bubble diameters, the films must be very thin, and that there is basically no gravitational flow through them, and thus negligible flowrates and amount of liquid contained inside them (when compared to the PBs and nodes). In the other limits, for large bubbles, with D well above 1 mm (meaning larger film areas, PB radius r, velocity and capillary number), the PB capillary suction is low, and falls in the range where slight variations of capillary pressure (thus of r) change the film thickness.[4,5] Moreover, the dynamic pressure in the liquid, arising from the flow, might no longer be negligible and can sustain such low PB suction. In that case, the situation becomes more complicated, and a coupling between the flow inside a PB and in a film is possible: a film can swell with increasing r (meaning decreasing P_c, and increasing v), and liquid circulation patterns have been observed.[32,33,47] Nevertheless, it is usually observed that circulation makes the liquid rise close to the PB, so that there is always a region or a line at $v = 0$ close to the PB–film connection. In addition, some pinching effects (where the film is locally very thin) at these film–PB connections have also been observed. Such effects have been studied theoretically,[54] as they are considered as possible precursor states for the occurrence of marginal regeneration.[55] So, in any case, despite that all the local hydrodynamics are not yet understood, considering $v = 0$ at point C appears realistic and consistent with all the observations. Moreover, even if it is recognized that film swelling can occur for large enough PB radii, the volume of liquid trapped in these films and the flowrate through them always remain low and negligible when compared to the PBs. On these issues, recent numerical simulations have compared flowrates in PBs and in thin films for any mobilities,[21] liquid fractions and film thicknesses. It is shown that, for a realistic case of ε of a few percent ($r \leqslant L$), the flow in the films can be important only if the surfaces are quite mobile and if the films are quite thick ($h \approx 10^{-2}L$), corresponding to conditions which are hardly fulfilled in a common foam (once looking at the observed ranges of variations of L, h or μ_s). In conclusion, as long as the liquid fraction is not extremely low ($\varepsilon \geqslant 10^{-3}$, or $r > 0.075\ L$) and the surface mobility is not very high ($M < 100$), it seems that the films can never be thick enough to contribute to foam drainage, and that liquid transport through them can thus be neglected, as done in the model and as confirmed by the agreement between the data and the model. But, it must be pointed out that the films are important since they control and induce the boundary condition at the PB corners C. Note though that the way the flow in a film is coupled to that inside its attached PB is still unclear.

On all these issues of balance between dissipation in PBs and nodes, it is interesting to note that the simplest or "most natural" conditions produced if one starts to investigate foam drainage (*i.e.* using commercial soap solutions made of low molecular weight surfactants, and with bubble diameters of approximately 1–3 mm) provide values of M right inside the crossover range. This is unfortunately the range where the contributions of nodes and PBs are close, where data analysis is the most complex, and where slight experimental changes allow to find one drainage regime or another. This might probably have been a reason why historically a unique and simple picture did not easily emerge from the experiments, and why apparently different sets of results were initially opposed.[9,16] When looking to these results in detail, it also finally seems that the observed differences were in fact due for the largest part to different bubble diameters, rather than to significantly different commercial surfactant solutions.

However, it is important to add that some experimental results do not fit with this picture, when varying bubble size or surfactant. In ref. 45,56, the case of foams of tiny bubbles, with $D < 0.3$ mm (or $L < 0.1$ mm) shows a behavior consistent with high interfacial mobility, while the parameter M is very low. This remains unexplained, and might be due to changes at the film–PB connections (studies of thin films of small areas

showed that different behaviors occur as the size is decreased[57]). It might also be due to the other bulk–surface coupling controlled by N which is expected to become strong as D decreases. But, quantitatively N is always quite small and its related effects should not be seen at these bubble diameters; note though that in thin film studies, effects linked to N occurred while N is also still quite small.[23] Nevertheless, these small bubble behaviors today remain unexplained. Also, in experiments with a single PB held on solid frames, some unexplained dependence of the surface viscosity on the flow rate Q has been observed (only at the lowest Q and PB radii), and which does not fit with the flow picture based on the mobility M.[32] In these experiments, the PB radius and liquid velocity are rather large, and the films attached to the PB swell in relation to the PB flow. The interesting point in this setup is that the film widths ($L \approx 1$ cm) are much bigger than the PB radius r ($r \approx 0.01$ cm): in that sense, it mimics a foam of extremely low liquid fraction, and as stated before and in ref. 21, this implies a liquid volume and flowrate in the films attached to the PB which might no longer be negligible. The observed effects at the lowest PB radii might thus be a first evidence of a regime where viscous dissipation within the films is dominating, eventually disappearing at higher Q as the PB volume increases. It is worth noting that such effects with Q are not found with another single PB setup (single vertical PB confined between glass plates[58]): similar PB radii and flowrates are studied, but the width of the film attached to the PB is much smaller here, and the data can be interpreted with a surface viscosity independent of Q.

2.4.2 Effect of the rheology of the surfactant solution. As shown in Section 2.2, the solution viscosity μ enters in M and N. Thus, the interfacial mobility should also be modified by μ, as it is by μ_s. The role of the bulk viscosity μ has been investigated, either with Newtonian or non-Newtonian fluids in 3D macroscopic foams,[59,60] and in single PBs.[32] At the limit of immobile surfaces, experiments with solutions containing glycerol at different concentrations have shown that the permeability K_c increases with M, and thus that the bulk–surface coupling is indeed also tunable by μ. But, the measured dependence of K_c with M does not follow the model exactly, assuming that glycerol does not modify the surface properties (which seems to be verified from interfacial measurements).[60] This discrepancy has also been seen in experiments on single PBs.[32] Here also, it is possible that the effects linked to N might be the relevant ones. It is worth noting that using μ to decrease the drainage rate is thus not as direct as one might think at first (looking only at the velocity scale v_0 given in Section 2.2), since K_c and K_n are also complex functions of μ (*via* their dependence on M or N).

The case of shear thinning fluids has also been investigated.[60] For these fluids, the viscosity decreases with the shear rate;[61] this is a very classical situation when polymers are added with surfactants.[61] It turns out that if one ascribes to each shear-thinning solution the viscosity value corresponding to the shear rate actually occurring into the foam (deduced from the average liquid velocity and PB radius), one recovers exactly the same results as for the Newtonian fluids.[60] Forced-drainage experiments have also been performed with polyethylene oxide (PEO) added to a surfactant solution.[59,60] Such a solution resists both shear and elongation strains.[61] The elongational viscosity μ_e of that solution is then much higher than the one of the Newtonian solution having the same shear viscosity. A curious result is reported in ref. 59,60: for the same shear viscosity, the foam made out of the PEO solution actually drains faster than the Newtonian one. This is surprising since the solution is expected to be as dissipative in shear, and more dissipative in elongation. This is confirmed by studies on Boger fluids (mixtures of PEO and glycerol, having constant μ and different μ_e). The interpretation of this result is not complete, and it is proposed that the tension-thickening character of the solution (the polymer modifies the flow in order to reduce elongation strains) could be important.[60]

Regarding the effects due to the properties of the foaming fluid, one must also report the experiments performed with magnetic foaming liquids. Surfactants have been added to ferrofluids to produce dispersed systems like foams or emulsions sensitive to magnetic fields. In ref. 62–64, results on 2D foams, on vertical thin films held on frames, and on columns of bubbles in tubes are reported, showing clear proof that the application of a magnetic field can modify the system properties.

2.5 Effect of the experimental conditions

Foam drainage does not only depend on the foam physical and chemical properties: especially for a freely draining foam, one also has to be careful of the effects of the experimental conditions, like the height or shape of the foam container, the number of bubbles at each height, or the initial vertical liquid distribution.

From the velocity defined in Section 2.2, in steady state, one can define a typical drainage timescale $t_d = H/v$, where H is the height of the foam. This gives the time required to drain 1/2 of the total foam liquid (this is valid for the channel-dominated regime; it is 2/3 in the node-dominated regime).[65] However, this is valid for containers having a constant cross section. Otherwise, if the cross section varies with height, the drainage curve (volume of drained liquid as a function of time) is changed. Theoretically, taking such a section variation into account can be done by considering the dependence of the number of PBs on the height $n(z)$. An interesting case is reported in ref. 66,67, for a container having a section which varies exponentially with height (similar to the Eiffel tower): in that case, it is predicted, and experimentally verified, that the liquid drains into the foam at the same rate everywhere, so that no vertical gradients are seen during the free-drainage. Also, in relation to froth flotation issues, the effect of the shape of the container (which increases with height in this case) has been discussed in ref. 68, and liquid fraction gradients have been computed along the vertical and horizontal axes.

In free-drainage, the height H of the sample does also matter. For a given ε and bubble diameter, the total volume of liquid spread in the foam is $V_{liq} = \varepsilon V_{foam}$, and $V_{foam} = HS$ (S is the foam sample section). For liquid to drain out, the bottom boundary conditions, $\varepsilon_c = 0.36$ and the equilibrium capillary profile over the typical height ξ, must be obtained; only once this wet layer is filled, is it possible to overcome the capillary

suction, and can liquid leak out. Note first that this process of "wetting" the foam bottom takes a certain delay time (determined in ref. 69), which depends on the bubble size and the initial liquid content, and during which no liquid drains out of the foam. Secondly, it is important to compare the volume V_{liq} to the volume of liquid required to fill the capillary holdup over ξ. It is possible that V_{liq} can be lower than this capillary holdup (for small H, small ε or both): in that case, the liquid will never leak out. Note that gravity still acts in the sense that a vertical gradient is produced (the bottom is wetter than the top), but no liquid gets out of the foam. This is the case for instance when studying low heights (typically less than 10 cm) of shaving foam; the very small bubble diameter, $D \approx 30$ μm, makes ξ quite large, while the initial liquid fraction is low, $\varepsilon \approx 0.07$.

Other experimental conditions are required to correctly perform free-drainage experiments, so that one gets conditions similar to the ones assumed in the models, without artefact. For instance, one must be careful that there are enough bubbles in the cross section, otherwise the contribution of the "surface PB" (also named "exterior PB") in contact with the wall container might become more important than that from the PBs inside the foam. Comparisons between the flow in "exterior" and "interior" PBs are given in ref. 21, as well as criteria for their relative importance. Again, as stated previously, the quality and uniformity of the foam is also important: at time zero, one should have no gaps or holes inside the foam and the liquid must be distributed evenly in the foam, and this usually requires a fast foam production process. If there are some initial vertical gradients of the liquid fraction, differences are found in the drainage curves.

Finally, it is possible to perform drainage experiments and to study fluid transport in a foam in cases where gravity is not the leading driving force. This can be done on the ground by studying liquid propagation in the direction orthogonal to gravity, but this remains limited in ε by convective instabilities.[70,71] Recently, experiments have been performed under microgravity conditions (during parabolic flights) initially with 2D foams (only one layer of bubbles between two plates),[72–74] and later in 3D foams.[75–77] The data have been compared to extensive simulations of liquid transport in microgravity.[78] These experiments allow evidencing of the capillary-induced liquid propagation, from areas of high liquid fraction to dryer ones. In Fig. 4c, transmission pictures of the foam during an imbibition experiment in microgravity are shown: liquid is injected in the cell center at a continuous flow rate Q into a dry foam (appearing white in the picture), as in a ground forced-drainage experiment. With time, the liquid propagates into the foam in a diffusive and isotropic way: as expected for a transport controlled by capillarity, the limit of the liquid propagation is a circle at any time.[77] From these experiments,[75–77] it also appears that when capillarity is the only driving force, the liquid front profile is much less sharp than on the ground; this seems to prevent convective instabilities, and to give access to high liquid fractions by such forced-drainage processes (ε can reach 0.4 in microgravity, whereas on the ground ε is limited to $\sim$0.2 because of the instabilities described previously). Thus, one might expect to get some new insights in these instabilities by these microgravity experiments, as well as with other new experiments related to this issue.[79,80] Quantitatively, comparison with the drainage models shows that they cannot explain the high ε range: these experiments have shown that the assumption made in the models, considering that all the liquid is only within the PBs, and describing dry foams, eventually fails as ε is increased. In fact, on the ground ε does not reach high enough values to find significant discrepancies, while for the high liquid fraction accessible in microgravity, clear discrepancies have been observed, mainly due to the fact that the node volume can no longer be neglected, typically as $\varepsilon > 0.15$.[77] Thus, experiments in microgravity also offer us some new data on foams at very high ε, useful for testing future models of the structure of very wet foams.

3 Coarsening

3.1 Physical concepts

With time, drainage is not the only process that occurs inside a foam. A foam also evolves by gas diffusion through the thin films from bubble to bubble.[1–3] Diffusion is due to pressure differences between bubbles, which can be evidenced by looking at the curvature of the bubble faces. For well separated droplets or grains, this process is known as Ostwald ripening, and is called "coarsening" for cellular materials, like foams. Coarsening thus tends to increase the volume of certain bubbles at the expense of others. On average, the net result is that the mean bubble diameter grows with time. There are still many unsolved issues on coarsening, regarding the dynamics of the growth of a single bubble, the possible universality obtained in the distribution of the bubble size with time, or the effects of the chemical components.

When investigating foam coarsening from the physicist's or mathematician's point of view, one usually considers extremely dry foam ($\varepsilon \approx 0$), zero thin film thickness, and with all the effects linked or due to the components included into a constant prefactor. Such studies, focusing on geometrical or topological aspects of coarsening, have dealt first with 2D foams (only one layer of bubbles), and more recently with 3D foams. The study of coarsening in 2D foams is simple to observe, simpler to model, and already a lot of results have been obtained. In 1952, von Neumann demonstrated that the time evolution of a 2D bubble depends only on the number of its sides, rather than on its size or shape.[81] The growth-rate of a bubble of area A and with n sides is: $dA/dt \propto (n - 6)$. For a hexagonal bubble with 6 sides, the area remains constant, whereas bubbles with $n < 6$ shrink, and bubbles with $n > 6$ expand. In Fig. 7, we show experimental pictures of a 2D foam

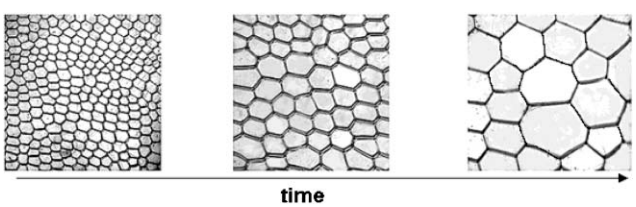

Fig. 7 2D foams at different times, illustrating coarsening. The arrow indicates the increase in time. The initial mean bubble diameter is $D = 1.5$ mm.

at different times. Bubbles with higher pressure and less than 6 edges shrink with time, and eventually vanish. Experimentally the von Neumann's law has been verified.[82–84] In addition, experiments, simulations and calculations for 2D foams now agree that a statistically scale invariant state exists (self-similarity). It means that the distributions of normalized bubble areas $A/\langle A(t)\rangle$ and face numbers remain invariant during coarsening. In this regime, the average bubble diameter scales in $t^{1/2}$, while the average area and bubble number vary as t and t^{-1}.

For 3D foams, theoretical works and simulations have been performed to try to find an analog to the von Neumann's law, and to determine whether or not the process is also self similar, with a scaling state regime asymptotically found. Here the bubble topology is determined by the number of bubble faces F (which replaces the number of sides n used in 2D), and one must also consider some averaging over the different bubble shapes having the same F. It turns out that the growth law for such average bubbles with F faces can be written:[85–87]

$$V_F^{-1/3}\partial V_F/\partial t = D_{\mathrm{eff}}G(F) \quad (6)$$

where V_F is the averaged volume of all bubbles with F faces in the foam, D_{eff} is a diffusion coefficient (depending on the components and discussed in Section 3.2), and G is a function of only F (with a neutral growth face number F_0 for which $G(F_0) = 0$). $G(F)$ is proportional to the integral of the mean curvature H of the bubble faces over the entire bubble surface. Different forms for $G(F)$ have been computed or calculated;[85–90] and the latest calculations showed that $G(F)$ is finally not a simple linear function of F,[90] in agreement with simulations using either large numbers of bubbles,[91] or small bubble clusters.[92] In any cases, all simulations show that F_0 is between 13 and 14.

Experimentally, studying coarsening in 3D is more complicated than in 2D (see next section). However some results can be compared with the predictions discussed above: for instance regarding the value F_0, some good agreement is found, starting from the pioneering work of Matzke,[93] and following with some tomographic studies.[94,95] In 3D, the coarsening process is also predicted to be scale invariant, with an average bubble diameter varying with $t^{1/2}$. On this point, experimentally, there are results obtained by optical methods of multiple light scattering, showing that scaling behaviors exist in foams.[96] This is also confirmed in a less direct way by rheological measurements, where one monitors the time evolution of the foam elastic modulus, which is inversely proportional to the bubble diameter.[97]

3.2 Role of the components in coarsening

As stated in the previous section, the effects on coarsening of the chemical components are included in the diffusion coefficient D_{eff} of eqn (6). With this coefficient, one must also consider a possible variation of the coarsening rate with the liquid fraction, not taken into account in Section 3.1. Starting from eqn (6), and considering that the net bubble growth corresponds to an effective mean curvature in the foam ($H \sim 1/\beta L$ (L is the PB length, and $\beta \approx 10$)), one obtains directly that $L\partial L/\partial t = D_{\mathrm{eff}}f(\varepsilon)$, where f is a function of ε discussed in detail below.[69] This is consistent with the scaling regime $L \sim t^{1/2}$, and allows us to define a coarsening time t_c: $t_c = L_0^2/(2D_{\mathrm{eff}}f(\varepsilon))$, with L_0 the PB length at $t = 0$. The way D_{eff} is supposed to depend on the properties of the chemicals was already discussed in ref. 98, and is given in detail in ref. 69:

$$D_{\mathrm{eff}} = \frac{4\delta_a}{3\delta_v\beta}\frac{D_F He\gamma v_m}{h} \quad (7)$$

In this model, γ is the surface tension, h is the thin film thickness (considered independent of ε and set by the PB capillary suction), and δ_a and δ_v are geometrical constants (also used in drainage to describe PB section and node shape). Linked to the gas, v_m is the ideal gas molar volume, D_F is the diffusivity of the gas inside the thin liquid films, and He is the gas Henry constant, reflecting the solubility of the gas. For the diffusivity in the film, one usually considers that it is the same as the one in the bulk. It is thus the product of diffusivity by solubility which is relevant for characterizing the effect of the gas. In fact, the Henry constant varies more than the diffusivity from one gas to another: D_F is always typically of the order of 10^{-5}–10^{-6} cm^2 s^{-1}, while He = 3.4 × 10^{-4} mol m^{-3} Pa^{-1} for CO_2, and is only 5.5 × 10^{-7} mol m^{-3} Pa^{-1} for a fluorinated gas like C_2F_6. Finally, all the effects of the liquid fraction are included in $f(\varepsilon)$: it is in fact a function describing the proportion of the bubble surface through which gas diffusion occurs. The exact form of this function is still under investigation. Some predictions have been made based on the idea that gas diffuses only through the thin films, and that their areas decrease as the PBs grow with ε, decorating and covering the bubbles more and more (see Fig. 2a). In that case, a first possible solution is (to the leading order): $f(\varepsilon) \sim (1 - (\varepsilon/\varepsilon_c)^{1/2})$,[99,100] while a slightly different form, $f(\varepsilon) \sim (1 - k\varepsilon^{1/2})^2$ (with $k = 1.52$), is proposed in ref. 69.

Experimental measurements of coarsening rates at controlled ε in 3D foams are scarce, mainly because they are difficult to perform. The main problem is to keep ε constant over long periods of time to get significant bubble size variation, and it becomes increasingly difficult as ε increases. Different approaches have been used to try to overcome the difficulty. Using a tall foam sample and during free-drainage, it is possible to investigate the coarsening at constant ε, at a position far from the top, during all the time it takes for the dry front to arrive at this position;[101] one can also create foams in steady-state by continuous gas bubbling;[102] performing forced-drainage at different foam ages has also been used;[100] lastly, one can try to avoid liquid fraction variations with a rotating cell setup, to alternatively invert the drainage direction in the sample, in order to keep ε constant in the cell center (details are given in ref. 103). In Fig. 8, some results obtained by this last method are shown: the relative variation of the PB length L, proportional to the bubble diameter, is measured by light transmission (in multiple scattering, $I_T \sim L$ for a constant ε). Results are given for $\varepsilon = 0.15$, with two different gases and for SDS foams and casein foams: they appear to be consistent with the scaling regime, $L \sim t^{1/2}$ at late times. From these data, one can then extract a coarsening time t_c, from which one gets D_{eff}. Note also that information on the dependence of the coarsening rate with ε can be inferred from draining foams, at a non-constant liquid fraction, but which

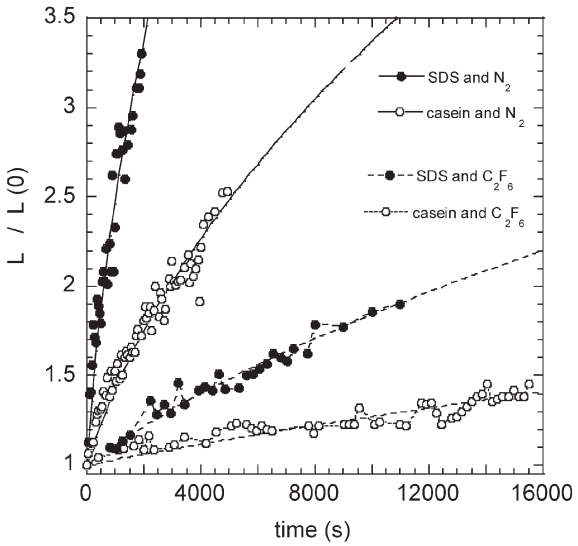

Fig. 8 Coarsening data at constant ε: $L(t)/L(t = 0)$ for foams made of solutions of SDS and casein, and for two different gases, N_2 and C_2F_6. For each system, the data can be fitted to extract a coarsening time t_c.

also undergo simultaneous coarsening.[69,101] In that case, it is then a matter of extracting data on coarsening *via* its effect on drainage (see also Section 4).

Experimentally, concerning the form of $f(\varepsilon)$, it is unfortunately still difficult today to draw definitive conclusions. From their measurements, Vera and Durian proposed a different scaling for $f(\varepsilon)$: $f(\varepsilon) \sim 1/\sqrt{\varepsilon}$.[101] However, in ref. 69, the form proposed seems to explain the experimental results. Nevertheless, it is worth noting that quantitatively all these results are in fact consistent, falling in the same range (especially for ε of a few percents, where all the forms of $f(\varepsilon)$ are almost equal). As well as for the results of Fig. 8, they can finally be used for *in situ* estimation of thin film thickness in a draining foam: values ranging between 30 to 60 nm are found for these experiments.[69,102,103] consistent with the range of bubble diameter used (which imply high capillary pressures, low capillary numbers, and thus thin films). It is however not clear if the thin film thickness h is constant with ε: for the small bubble sizes used in these experiments, the relative agreement between data and model tends to show that h does not change with ε, especially in an intermediate range of ε. However, for very wet foams ($\varepsilon < 0.01$) or very dry ones ($\varepsilon > 0.15$), the observed discrepancies might come from a dependence of h on ε. As discussed in Section 2, for large bubble diameter D bigger than a few mm, the low capillary pressures in the foam allow some coupling between flow in PBs and films, and there h varies much more with ε.[33] Lastly, it is interesting to add that the coarsening time is not always decreased as h is decreased: experimental results have been reported showing that the permeability of a Newton black film—where the two surfactant layers are in contact, and h is only a few nm—is surprisingly lower than that of a thicker film, still containing fluid between the two bubble interfaces.[104,105]

Regarding the effect of the gas, the results shown in Fig. 8 for N_2 and C_2F_6 are consistent with the model: considering all the other parameters as constant, the ratio of the two measured coarsening times t_c is equal to the ratio of the gas properties. More interesting is the behavior with gas mixtures. In that case, one must not only consider the pressure differences between bubbles, but also the partial pressures of each gas. It has been shown that only a few percent of a "slow diffusing" gas A, mixed with a "fast diffusing" gas B, can already strongly reduce the coarsening rate.[106,107] As the fast diffusion of B occurs, it modifies the relative concentrations of A and B in the bubbles; such changes consequently modify the partial pressures. As a matter of fact, only small variations of the concentration of A are needed to bring to equilibrium the partial pressures of B, and thus to stop its diffusion. Thus, after a rapid equilibration of the partial pressure of B, the foam coarsens almost as if it was made of the slowly diffusing gas A (even though the initial volume fraction of gas A is only a few percent). Note that a special situation is predicted when only a tiny amount of a "slow diffusing" gas A is added (volume fraction of gas A $< 10^{-5}$): the foam then should coarsen in a non self similar way, with its polydispersity widely increasing, and with coexisting small and large bubbles.[106] Also, due to gas partial pressure differences, a curious effect has been reported when a foam made of a "slow diffusing" gas (C_2F_6 for instance) is put into contact with an outside gas more soluble (as air).[108] Despite the fact that the total pressure inside the bubbles is always higher than the outside pressure, the air enters the foam (where its partial pressure is zero), and makes the foam expand, like a souffle. During this process, bubbles with a low number of faces (less than 10) grow in volume, while they should normally shrink. As a proof that this foam expansion is due to the outside gas entering into the foam, the effect vanishes when the same gas is used inside and outside the foam.

Concerning the role of the surfactants in coarsening, it is first clear that the components play a role *via* the surface tension γ, but also *via* the thin film thickness h; this equilibrium thickness is the result of interaction between the surfactant layers adsorbed on the bubble interfaces. In that sense, it must also depend on the presence of additives in the bulk (like salt or polymers), which modify the interaction potential. As noted previously, the possibility for a surfactant system to make or not stable Newton black films (under high capillary pressures, like in extremely dry foams) is also an important point which might modify the coarsening rate. To illustrate these points, in Fig. 8, it is shown that a casein foam coarsens approximately 5–7 times slower than an SDS foam (for the same liquid fraction and initial bubble diameters). Surface tensions are similar, and cannot explain the difference. However video-microscopy studies of single thin films show that the equilibrium thin film thickness with casein is about 5–7 times greater than for SDS.[103] Thus here, the observed difference might only be due to the thickness h, and no other effects due to the proteins layers or to their viscoelasticity have to be invoked to explain these coarsening rates. Following how single bubbles sitting just below a liquid–air interface shrink with time (as the gas escapes to the outside), it has been shown that for a protein like β-casein no corrections due to surface viscoelasticity are required; however, for other systems (like β-lactoglobulin) one must introduce a small surface elasticity to better describe the data.[109,110] The possible role of interfacial and bulk rheological properties is also discussed

theoretically in ref. 111–114. In fact, for low molecular weight surfactants usually used for foams, it seems that it is not necessary to take such effects into account. On the contrary, recent experiments with solid particles adsorbed at interfaces show that the dynamics can be strongly reduced and even arrested,[115,116] especially as these particles are often irreversibly attached to the surfaces and thus get more and more packed and jammed as bubbles or droplets shrink.[117] On all these coarsening issues, more experiments are needed, to allow us to investigate the details of the process. In that sense, X-ray tomography (using synchrotron sources) is a promising technique.[118]

4 Coupling between coarsening and drainage

While a foam is freely draining, it might be simultaneously coarsening. One can use κ = drainage time t_d/coarsening time t_c, to determine the importance of coarsening during drainage:[69]

$$k = \frac{4\mu H D_{\text{eff}} f(\varepsilon)}{K\rho g \varepsilon D^4} \quad (8)$$

Here the equation is given for the case of low interfacial mobility (the other limit is given in ref. 69). If κ is small, there is no coarsening during drainage, the bubble diameter is constant during the whole process and thus the models and results shown in Section 2 and 3 are valid. On the contrary, for high values of κ, the bubble diameter strongly varies during drainage, and the drainage dynamics is finally accelerated by this simultaneous coarsening. Despite the decrease of ε, the coarsening makes the PB length bigger with time, increasing the liquid velocity (see eqn (2) and (3)). In the same time, as the foam drains, the coarsening rate increases and the bubble growth gets even faster, implying faster and faster liquid velocities. As a result of these coupled effects, the drainage time can be strongly reduced by coarsening. Examples of such effects are shown in Fig. 9: drainage curves (volume of drained liquid, normalized by the final drained volume, as a function of time) for two gases (N_2 and C_2F_6) are reported (SDS foams); the foam height is 30 cm, the initial bubble diameter D = 0.2 mm, and two initial liquid fractions ε = 0.04 and 0.25 are used. Clearly, with N_2, coarsening occurs during drainage, and the resulting drainage time is much smaller than with C_2F_6. In that extreme case of strong coarsening, it has been predicted and observed that the volume of drained liquid first follows a quadratic behavior.[44,69] Also, the dependence on ε is expected to vanish (as seen in Fig. 9), and a self-limiting drainage is observed.[44,69] On the contrary, for C_2F_6, where the foam undergoes no coarsening during drainage ($\kappa < 1$) there is a clear dependence of the drainage time on ε; note that one can also see the delay time discussed in Section 2.5 during which no liquid leaks out of the foam for the dry case (due to smaller fluid velocity).

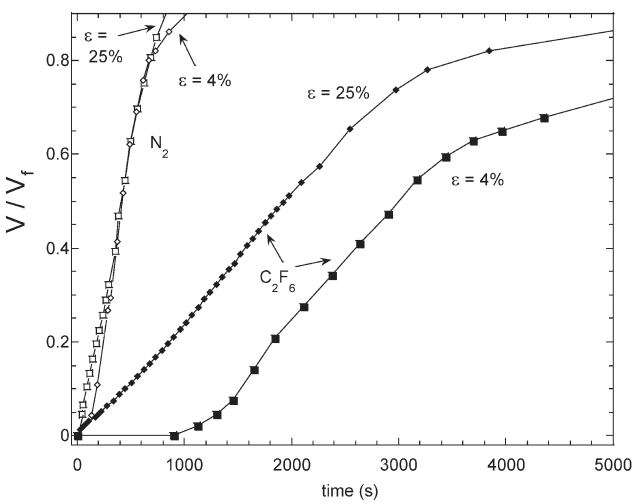

Fig. 9 Free-drainage curves for dry and wet SDS foams, made of two different gases, N_2 and C_2F_6. When coarsening proceeds simultaneously with drainage (N_2), drainage is accelerated, and the variation with ε vanishes.

The value of κ can be controlled by many parameters: firstly, it strongly depends on the bubble diameter D, and on the gas properties. So, as seen before, the gas controls the coarsening rate, but it turns out that it can also modify the drainage rate. Lastly, one can again point out the role of the foam height H. The case of small H was discussed in Section 2.5; here it appears that as H increases, one might expect a drainage more and more controlled by coarsening, as shown in ref. 65 where it is reported that the dependence of the drainage time on ε vanishes with increasing height. However, not everything is understood regarding the mechanism of this drainage–coarsening coupling. In ref. 69, a simple time-dependent bubble size is added into the usual drainage equation, while Vera and Durian proposed that one should also take into account an extra liquid flow downward, resulting from an upward gas transport due to coarsening (from the bottom small bubbles to the large ones at the top, see Fig. 1).[101]

5 Conclusions and outlook

Experimental results have been collected in the last years allowing us to determine more and more accurately the role of foam components (surfactant, liquid and gas) on drainage and coarsening. In addition, the effects of the bubble size and liquid fraction are also better known and understood, and it is becoming possible to compare these ''physical'' effects to the ''chemical'' ones. In a simplified and rough picture, one can conclude that the physical chemistry of the components usually matters and cannot be ignored; however, one must also add that the main drainage and coarsening features actually depend so strongly on the physical parameters (D and ε), that these parameters can be seen as the most important ones. For instance, with drainage, it is recognized now that an important factor is the coupling between the bulk and surface flows in the PBs and nodes, and that this is tunable by the surfactant and the liquid viscosity. So, physical chemistry matters, but such effects remain ultimately small: the liquid velocity is actually much more varied by changing the bubble size than the surface shear viscosity. However, this is not always as simple, and the effect of the gas on drainage is a good example: *via* the coupling between drainage and coarsening, the gas can also strongly alter the drainage rates.

In a large range of experimental conditions, a quantitative agreement is found on drainage between models and experiments, when using the mobility parameter M. Nevertheless, not all the observations are explained, especially for very small bubbles, and regarding the dependence on bulk viscosity. Also, for coarsening, experimental results are providing some understanding of the role of the chemistry, but many questions still remain unanswered, especially because studying coarsening at constant ε remains experimentally difficult. Moreover, bubble growth by film rupturing is even less studied and remains very poorly understood, some works by recording the sound emitted by the collapse of a foam showing some avalanche effects.[119]

With all these new findings, our understanding of foam aging has increased, and one can think now about means of producing new reactive foams through controlled aging, or with aging dynamics going along non classical paths. One can also start to investigate more complex issues, like the structure and properties of very wet foams ($\varepsilon > 0.2$), or the problem of drainage during foam growth and collapse,[120] or even issues linked to solid or metallic foams where both drainage and solidification occurs simultaneously.[121,122] Also, knowing about foam aging is crucial for understanding foam rheology; for instance, coarsening plays an important role in the low frequency rheological response of a foam.[97] Lastly, it is worth noting that rheology is another topic where the same question of the balance between physical and chemical parameters is starting to be addressed (concerning the friction on solid substrates for instance,[123,124] or the flow uniformity under steady-shear[125]).

Many aspects of foam aging are also valid for emulsion aging (dispersions of one liquid into another, stabilized by surfactants as foams[126]). For emulsions, gravity also tends to separate the two fluids (it is called ''creaming'' rather than ''drainage''). Note though that emulsion creaming can be quite a bit slower and less critical than foam drainage, as the density variations between two fluids can be much lower (creaming can even be completely removed by matching the fluid density[127]). Also, coarsening by diffusion, similar to that described here for foams, is also observed; it must be noticed that the study of droplet growth by film rupturing is more investigated and understood in emulsions than in foams.[128–130]

Acknowledgements

The French space agency (CNES) and the European space agency (ESA) are acknowledged for financial support. The author also thanks D. J. Durian for the picture of Fig. 1, W. Drenckhan and A. Saugey for the simulations shown in Fig. 3, and all of these scientists for sharing unpublished results.

References

1 R. K. Prud'homme and S. Khan, *Foams: Theory, Measurements, and Applications*, Marcel Dekker Inc., New York, 1997.
2 D. Weaire and S. Hutzler, *The physics of foams*, Oxford University Press, New York, 1999.
3 A. Saint-Jalmes, D. Durian and D. Weitz, *Kirk-Othmer Encyclopedia of Chemical Technology*, 5th edn, 2005, vol. 12, p. 1.
4 V. Bergeron, *J. Phys.: Condens. Matter*, 1999, **11**, R215.
5 C. Stubenrauch and R. von Klitzing, *J. Phys.: Condens. Matter*, 2003, **15**, R1197.
6 Y. Jayalakshmi, L. Ozanne and D. Langevin, *J. Colloid Interface Sci.*, 1995, **170**, 358.
7 S. Cox, D. Weaire, S. Hutzler, J. Murphy, R. Phelan and G. Verbist, *Proc. R. Soc. London, Ser. A*, 2000, **456**, 2441.
8 S. A. Koehler, S. Hilgenfeldt and H. A. Stone, *Langmuir*, 2000, **16**, 6327.
9 D. Weaire, S. Hutzler, S. Cox, N. Kern, M. A. Alonso and W. Drenckhan, *J. Phys.: Condens. Matter*, 2003, **15**, S65.
10 H. A. Stone, S. A. Koehler, S. Hilgenfeldt and M. Durand, *J. Phys.: Condens. Matter*, 2003, **15**, S283.
11 I. Gol'dfarb, K. Khan and I. Shreiber, *Fluid Dyn.*, 1988, **23**, 244.
12 G. Verbist and D. Weaire, *Europhys. Lett.*, 1994, **26**, 631.
13 G. Verbist, D. Weaire and A. Kraynik, *J. Phys.: Condens. Matter*, 1996, **8**, 3715.
14 D. Weaire, S. Hutzler, G. Verbist and E. Peters, *Adv. Chem. Phys.*, 1997, **102**, 315.
15 A. Bhakta and E. Ruckenstein, *Adv. Colloid Interface Sci.*, 1997, **70**, 1.
16 S. A. Koehler, S. Hilgenfeldt and H. A. Stone, *Phys. Rev. Lett.*, 1999, **82**, 4232.
17 S. Cox, G. Bradley, S. Hutzler and D. Weaire, *J. Phys.: Condens. Matter*, 2001, **13**, 4863.
18 R. Leonard and R. Lemlich, *AIChE J.*, 1965, **11**, 18.
19 D. Desai and R. Kumar, *Chem. Eng. Sci.*, 1982, **37**, 1361.
20 A. Nguyen, *J. Colloid Interface Sci.*, 2002, **249**, 194.
21 S. Koehler, S. Hilgenfeldt and H. Stone, *J. Colloid Interface Sci.*, 2004, **276**, 420.
22 M. Durand and D. Langevin, *Eur. Phys. J. E*, 2002, **7**, 35.
23 G. Singh, G. Hirasaki and C. Miller, *J. Colloid Interface Sci.*, 1996, **184**, 92.
24 S. Stoyanov and N. Denkov, *Langmuir*, 2001, **17**, 1150.
25 D. Weaire, N. Pittet, S. Hutzler and D. Pardal, *Phys. Rev. Lett.*, 1993, **71**, 2670.
26 S. Hutzler, D. Weaire and R. Crawford, *Europhys. Lett.*, 1998, **41**, 461.
27 M. Vera, A. Saint-Jalmes and D. Durian, *Phys. Rev. Lett.*, 2001, **84**, 3001.
28 D. Weaire and S. Hutzler, *Philos. Mag. B*, 2003, **83**, 2747.
29 S. Marze, A. Saint-Jalmes and D. Langevin, *Colloids Surf., A*, 2005, **263**, 121.
30 S. Koehler, S. Hilgenfeldt, E. Weeks and H. Stone, *Phys. Rev. E: Stat., Nonlinear, Soft Matter Phys.*, 2002, **66**, 040601(R).
31 S. Koehler, S. Hilgenfeldt, E. Weeks and H. Stone, *J. Colloid Interface Sci.*, 2004, **276**, 439.
32 O. Pitois, C. Fritz and M. Vignes-Adler, *Colloids Surf., A*, 2005, **261**, 109.
33 O. Pitois, C. Fritz and M. Vignes-Adler, *J. Colloid Interface Sci.*, 2005, **282**, 458.
34 W. Drenckhan, S. Gatz and D. Weaire, *Phys. Fluids*, 2004, **16**, 3115.
35 M. Vera, A. Saint-Jalmes and D. J. Durian, *Appl. Opt.*, 2001, **40**, 4210.
36 A. S. Gittings, R. Bandyopadhyay and D. J. Durian, *Europhys. Lett.*, 2004, **65**, 414.
37 D. Weaire, S. Findlay and G. Verbist, *J. Phys.: Condens. Matter*, 1995, **7**, L217.
38 R. Phelan, D. Weaire, E. Peters and G. Verbist, *J. Phys.: Condens. Matter*, 1996, **8**, L475.
39 S. Hutzler, G. Verbist, D. Weaire and J. van der Steen, *Europhys. Lett.*, 1995, **31**, 497.
40 K. Feitosa, S. Marze, A. Saint-Jalmes and D. J. Durian, *J. Phys.: Condens. Matter*, 2005, **17**, 6301.
41 J. DiMeglio and P. Baglioni, *J. Phys.: Condens. Matter*, 1994, **6**, A375.
42 M. Durand, G. Martinoty and D. Langevin, *Phys. Rev. E: Stat., Nonlinear, Soft Matter Phys.*, 1999, **60**, R6307.
43 S. Neethling, H. Lee and J. Cilliers, *J. Phys.: Condens. Matter*, 2002, **14**, 331.
44 A. Saint-Jalmes and D. Langevin, *J. Phys.: Condens. Matter*, 2002, **14**, 9397.
45 A. Saint-Jalmes, Y. Zhang and D. Langevin, *Eur. Phys. J. E*, 2004, **15**, 53.

46 A. Martin, K. Grolle, M. Bos, M. Cohen-Stuart and T. van Vliet, *J. Colloid Interface Sci.*, 2002, **254**, 175.
47 V. Carrier, S. Destouesse and A. Colin, *Phys. Rev. E: Stat., Nonlinear, Soft Matter Phys.*, 2002, **65**, 061404.
48 N. F. Djabbarah and D. Wasan, *Chem. Eng. Sci.*, 1982, **37**, 175.
49 J. Petkov, K. Danov, N. Denkov, R. Aust and F. Durst, *Langmuir*, 1996, **12**, 2650.
50 N. Vilkova and P. Kruglyakov, *Colloids Surf., A*, 2005, **263**, 205.
51 G. Bantchev and D. Schwartz, *Langmuir*, 2003, **19**, 2673.
52 C. Barentin, P. Muller, C. Ybert, J. Joanny and J. DiMeglio, *Eur. Phys. J. E*, 2000, **2**, 153.
53 F. Bouchama and J. DiMeglio, *J. Phys.: Condens. Matter*, 1996, **8**, 9525.
54 A. Aradian, E. Raphael and P. DeGennes, *Europhys. Lett.*, 2001, **55**, 834.
55 K. Mysels, K. Shinoda and S. Frenkel, *Soap films, studies of their thinning*, Pergamon press, London, 1959.
56 A. Cervantes-Martinez, A. Saint-Jalmes, A. Maldonado and D. Langevin, *J. Colloid Interface Sci.*, 2005, **14**, 9397.
57 O. Velev, G. Constandinides, D. Avraam, A. C. Payatakes and R. Borwankar, *J. Colloid Interface Sci.*, 1995, **175**, 68.
58 W. Drenckhan, A. Saugey, P. McGuiness, D. Weaire, H. Ritacco, A. Saint-Jalmes and D. Langevin, *Phys. Fluids*, submitted.
59 M. Safouane, M. Durand, A. Saint-Jalmes, D. Langevin and V. Bergeron, *J. Phys. IV*, 2001, **11**, Pr6–275.
60 M. Safouane, A. Saint-Jalmes, V. Bergeron and D. Langevin, *Eur. Phys. J. E*, 2006, **19**, 195.
61 H. Barnes, J. Hutton and K. Walters, *An introduction to rheology*, Elsevier, Amsterdam, 1989.
62 F. Elias, C. Flament, J. Bacri, O. Cardoso and F. Graner, *Phys. Rev. E: Stat., Nonlinear, Soft Matter Phys.*, 1997, **56**, 3310.
63 F. Elias, J. Bacri, C. Flament, E. Janiaud, D. Talbot, W. Drenckhan, S. Hutzler and D. Weaire, *Colloids Surf., A*, 2005, **263**, 65.
64 W. Drenckhan, F. Elias, S. Hutzler, D. Weaire and E. Janiaud, *J. Appl. Phys.*, 2003, **93**, 10078.
65 A. Saint-Jalmes, M. Vera and D. J. Durian, *Eur. Phys. J. B*, 1999, **12**, 67.
66 A. Saint-Jalmes, M. Vera and D. J. Durian, *Europhys. Lett.*, 2000, **50**, 695.
67 A. Saint-Jalmes and D. J. Durian, *Europhys. Lett.*, 2001, **55**, 447.
68 P. Grassia and S. Neethling, *Colloids Surf., A*, 2004, **263**, 165.
69 S. Hilgenfeldt, S. A. Koehler and H. A. Stone, *Phys. Rev. Lett.*, 2001, **86**, 4704.
70 S. Koehler, S. Hilgenfeldt and H. Stone, *Europhys. Lett.*, 2000, **54**, 335.
71 S. Hutlzer, S. Cox and G. Wang, *Colloids Surf., A*, 2005, **263**, 178.
72 D. Noever and R. Cronise, *Phys. Fluids*, 1994, **6**, 2493.
73 H. Caps, H. Decauwer, M.-L. Chevalier, G. Soyez, M. Ausloos and N. Vandewalle, *Eur. Phys. J. B*, 2003, **33**, 115.
74 H. Caps, S. Cox, H. Decauwer, D. Weaire and N. Vandewalle, *Colloids Surf., A*, 2005, **261**, 131.
75 A. Saint-Jalmes, S. Marze, M. Safouane and D. Langevin, *Microgravity Sci. Technol.*, 2006, **18**, 5.
76 A. Saint-Jalmes, S. Marze, M. Safouane, D. Langevin, S. Cox and D. Weaire, *Microgravity Sci. Technol.*, 2006, in press.
77 A. Saint-Jalmes, S. Marze, H. Ritacco, D. Langevin, S. Bail, J. Dubail, L. Guingot, G. Roux, P. Sung and L. Tosini, *Phys. Rev. Lett.*, 2006, submitted.
78 S. Cox and G. Verbist, *Microgravity Sci. Technol.*, 2003, **14**, 45.
79 S. Cox, M. A. Alonso, D. Weaire and S. Hutzler, *Eur. Phys. J. E*, 2006, **19**, 17.
80 S. Hutzler, N. Peron, D. Weaire and W. Drenckhan, *Eur. Phys. J. E*, 2004, **14**, 381.
81 J. von Neumann, *Metal Interfaces*, American Society for Metals, Cleveland, 1952, p. 108.
82 J. Glazier, S. Gross and J. Stavans, *Phys. Rev. A*, 1987, **36**, 306.
83 J. Glazier and J. Stavans, *Phys. Rev. A*, 1989, **40**, 7398.
84 J. Stavans and J. Glazier, *Phys. Rev. Lett.*, 1989, **62**, 1318.
85 W. Mullins, *J. Appl. Phys.*, 1986, **59**, 1341.
86 W. Mullins, *Acta Metall.*, 1989, **37**, 2979.
87 J. Glazier, *Phys. Rev. Lett.*, 1993, **70**, 2170.
88 N. Rivier, *Philos. Mag. B*, 1983, **47**, 91.
89 F. Wakai, N. Enomoto and H. Ogawa, *Acta Mater.*, 2000, **48**, 1297.
90 S. Hilgenfeldt, A. Kraynik, S. Koehler and H. Stone, *Phys. Rev. Lett.*, 2001, **86**, 2685.
91 A. M. Kraynik, D. Reinelt and F. van Swol, in *Proceedings of the XIIIth International Congress on Rheology*, ed. D. M. Bindings *et al.*, Cambridge, UK, 2000, p. 1.
92 S. Jurine, S. Cox and F. Graner, *Colloids Surf., A*, 2005, **263**, 18.
93 E. Matzke, *Am. J. Bot.*, 1946, **33**, 58.
94 C. Monnereau, B. Prunet-Foch and M. Vignes-Adler, *Phys. Rev. E: Stat., Nonlinear, Soft Matter Phys.*, 2001, **63**, 061402.
95 C. Monnereau and M. Vignes-Adler, *Phys. Rev. Lett.*, 1998, **80**, 5228.
96 D. J. Durian, D. Weitz and D. Pine, *Phys. Rev. A*, 1991, **44**, R7902.
97 R. Hohler and S. Cohen-Addad, *J. Phys.: Condens. Matter*, 2005, **17**, R1041.
98 H. Princen and S. Mason, *J. Colloid Sci.*, 1965, **20**, 353.
99 F. Bolton and D. Weaire, *Philos. Mag. B*, 1991, **63**, 795.
100 S. Hutzler and D. Weaire, *Philos. Mag. Lett.*, 2000, **80**, 419.
101 M. Vera and D. J. Durian, *Phys. Rev. Lett.*, 2002, **88**, 088304.
102 K. Feitosa and D. J. Durian, 2006, private communication.
103 A. Saint-Jalmes, M. Peugeot, H. Ferraz and D. Langevin, *Colloids Surf., A*, 2005, **263**, 219.
104 R. Krustev, D. Platikanov and M. Nedyalkov, *Colloids Surf., A*, 1993, **79**, 129.
105 R. Krustev, D. Platikanov and M. Nedyalkov, *Colloids Surf., A*, 1997, **123**, 383.
106 D. Weaire and V. Pageron, *Philos. Mag. Lett.*, 1990, **62**, 417.
107 F. Gandolfo and H. Rosano, *J. Colloid Interface Sci.*, 1997, **194**, 31.
108 G. Maurdev, A. Saint-Jalmes and D. Langevin, *J. Colloid Interface Sci.*, 2006, **300**, 735.
109 E. Dickinson, R. Ettelaie, B. Murray and Z. Du, *J. Colloid Interface Sci.*, 2002, **252**, 202.
110 R. Ettelaie, E. Dickinson, Z. Du and B. Murray, *J. Colloid Interface Sci.*, 2003, **263**, 47.
111 A. Ronteltap, B. Damste, M. de Gee and A. Prins, *Colloids Surf.*, 1990, **47**, 269.
112 A. Ronteltap and A. Prins, *Colloids Surf.*, 1990, **47**, 285.
113 M. Fyrillas, W. Kloek, T. V. Vliet and J. Mellema, *Langmuir*, 2000, **16**, 1014.
114 W. Kloek, T. von Vliet and M. Meinders, *J. Colloid Interface Sci.*, 2001, **237**, 158.
115 Z. Du, M. Bilbao-Montoya, B. Binks, E. Dickinson, R. Ettelaie and B. Murray, *Langmuir*, 2003, **19**, 3106.
116 S. Arditty, C. Whitby, B. Binks, V. Schmidtt and F. Leal-Calderon, *Eur. Phys. J. E*, 2003, **11**, 273.
117 A. B. Subramaniam, M. Abkharian, L. Mahadevan and H. Stone, *Nature*, 2005, **438**, 930.
118 J. Lambert, I. Cantat, R. Delannay, A. Renault, F. Graner, J. Glazier, I. Veretennikov and P. Cloetens, *Colloids Surf., A*, 2005, **263**, 295.
119 W. Muller and J. DiMeglio, *J. Phys.: Condens. Matter*, 1999, **11**, L209.
120 S. Neethling, H. Lee and P. Grassia, *Colloids Surf., A*, 2005, **263**, 184.
121 S. Cox, G. Bradley and D. Weaire, *Eur. Phys. J.: Appl. Phys.*, 2001, **14**, 87.
122 O. Brunke, A. Hamann, S. Cox and S. Odenbach, *J. Phys.: Condens. Matter*, 2005, **17**, 6353.
123 N. D. Denkov, S. Tcholakova, K. Golemanov, V. Subramanian and A. Lips, *Colloids Surf., A*, 2006, **282**, 329.
124 A. Saugey, W. Drenckhan and D. Weaire, *Phys. Fluids*, 2006, **18**, 053101.
125 L. Becu, S. Manneville and A. Colin, *Phys. Rev. Lett.*, 2006, **96**, 138302.
126 P. Becher, *Encyclopedia of Emulsion Technology*, Marcel Dekker, New York, 1985.
127 M. Robins, A. Watson and P. Wilde, *Curr. Opin. Colloid Interface Sci.*, 2002, **7**, 419.
128 F. Leal-Calderon and P. Poulin, *Curr. Opin. Colloid Interface Sci.*, 1999, **4**, 223.
129 V. Schmitt and F. Leal-Calderon, *Europhys. Lett.*, 2004, **67**, 662.
130 V. Schmitt, C. Cattelet and F. Leal-Calderon, *Langmuir*, 2004, **20**, 46.